Atmospheric Environment 92 (2014) 76–86

Contents lists available at ScienceDirect

Atmospheric Environment

journal homepage: www.elsevier.com/locate/atmosenv

A multi-year evolution of aerosol chemistry impacting visibility and haze formation over an Eastern Asia megacity, Shanghai

Yanfen Lin [a,d], Kan Huang [a,c,**], Guoshun Zhuang [a,b,*], Joshua S. Fu [c], Qiongzhen Wang [a,b], Tingna Liu [a,b], Congrui Deng [a,b], Qingyan Fu [a,d]

[a] Center for Atmospheric Chemistry Study, Department of Environmental Science and Engineering, Fudan University, Shanghai 200433, PR China
[b] Shanghai Key Laboratory of Atmospheric Particle Pollution and Prevention (Lap^3), Shanghai 200433, PR China
[c] Department of Civil and Environmental Engineering, The University of Tennessee, Knoxville, TN 37996, USA
[d] Shanghai Environmental Monitoring Center, Shanghai 200030, China

HIGHLIGHTS

- Visibility and haze frequency were not improved in Shanghai during 2004–2008.
- Haze caused by secondary inorganic pollution induced the lowest visibility.
- $CaSO_4$ and $Ca(NO_3)_2$ in aerosol were gradually replaced by $(NH_4)_2SO_4$ and NH_4NO_3.
- Evolution of aerosol chemical species caused negligible improvement of visibility.

ARTICLE INFO

Article history:
Received 4 December 2013
Received in revised form
4 April 2014
Accepted 7 April 2014
Available online 12 April 2014

Keywords:
Haze
Visibility trend
Chemical species
Aerosol evolution
Ammonium salts

ABSTRACT

A multi-year (2004–2008) study of horizontal visibility and factors controlling its variations was conducted in Shanghai. The seasonal average visibility in spring, summer, autumn, and winter was 7.7 km, 8.4 km, 8.1 km, and 6.5 km, respectively, significantly exceeding the haze criteria of 10 km throughout all four seasons. Although SO_2 and NO_2 concentrations gradually shifted to lower levels on an annual basis, no distinct improvement of the annual mean visibility was noticed. Via a grouping method, it was found that the water soluble ions and black carbon were the major contributors to haze formation while the role of mineral aerosol was negligible. Of the ions, SO_4^{2-}, NO_3^-, NH_4^+, K^+, and $C_2O_4^{2-}$ were most associated with the formation of heavy haze. SO_4^{2-} and NO_3^- were both found to have significant decreasing trends with annual decreasing rates of 0.96 and 0.56 μg/m^3/yr, respectively. Conversely, NH_4^+ showed a significant increasing trend with the annual increasing rate of 0.52 μg/m^3/yr. Based on a quantitative correlation analysis, the roles of NH_4^+ and Ca^{2+} on the acids neutralization were almost equivalent in the earlier years of 2004–2005. While the role of Ca^{2+} had tremendously dropped to less than 23% in the later years of 2006–2008. Intense control measures on the emissions of construction works and roadside dust were the main driving force for the evident decreasing trend of annual Ca^{2+} concentrations. This study found that the gradual replacement of $CaSO_4$ and $Ca(NO_3)_2$ by $(NH_4)_2SO_4$ and NH_4NO_3 in aerosol was the major cause of no improvement of the visibility impairment in Shanghai during recent years.

1. Introduction

Haze is an apparent symptom of visibility degradation. The major contributors to haze, e.g. the gaseous precursors and particulate matter, have attracted intensive interests due to its impact on cloud formation, public health, agriculture, and even global climate change (Chen et al., 2003; Kang et al., 2004; Schichtel et al., 2001). The formation of haze is closely related to atmospheric pollution and meteorological factors (Watson, 2002). Generally, haze forms from both excessive primary aerosol emitted

* Corresponding author. Shanghai Key Laboratory of Atmospheric Particle Pollution and Prevention (Lap^3), Shanghai 200433, PR China.
** Corresponding author. Center for Atmospheric Chemistry Study, Department of Environmental Science and Engineering, Fudan University, Shanghai 200433, PR China.
E-mail addresses: khuang7@utk.edu (K. Huang), gzhuang@fudan.edu.cn (G. Zhuang).

http://dx.doi.org/10.1016/j.atmosenv.2014.04.007
1352-2310/

from anthropogenic sources and the gas-to-particle transformed second aerosol (Chameides et al., 1999; Watson, 2002). The effect of emissions-controls on visibility in southern California was simulated and it was found that the secondary aerosol species were the major cause of significant visibility reduction (Kleeman et al., 2001). Kang et al. (2004) investigated the chemical characteristics of acidic gas pollutants and $PM_{2.5}$ species during hazy episodes in Seoul, South Korea. They found that major ionic species, NO_3^-, SO_4^{2-}, and NH_4^+, and organic materials were the two biggest contributors to $PM_{2.5}$. Chen et al. (2003) studied the summer haze in the mid-Atlantic region. They observed high fractions of SO_4^{2-} (~60%) and signified the role of SO_4^{2-} in haze formation.

Marked decline of visibility and increase of the occurrence frequency of haze have been recorded over many urban areas in developed countries from the 1960s to 1980s (Cass, 1979; Vinzani and Lamb, 1985). Great efforts have been made to reduce the emissions to improve the visibility during the past several decades. It was reported that the visibility improved due to the reduction of pollutant emissions in the United States and Europe since the 1980s (Wang et al., 2009). Schichtel et al. (2001) investigated patterns and trends of haze over the United States from 1980 to 1995 and found that the haze decline was consistent with reductions of $PM_{2.5}$ and sulfur emissions. A massive decline (about 50% in 30 years) of low-visibility occurrences during the past 30 years throughout Europe was also found, and the decline was spatially and temporally correlated with trends in sulfur dioxide emissions (Vautard et al., 2009).

Based on the long-term remote sensing products from SeaWiFS from January 1998 to December 2010, the annual trends of AOD (Aerosol Optical Depth, 550 nm) at both global and regional scales were compared (Hsu et al., 2012). Except for the Arabian Peninsula, which was mainly impacted by dust, the three regions of China (i.e. northern, southern, and eastern) showed the largest positive trends affected by the human activities throughout the world. Visibility degradation has spread over not only the industrial and populous areas in China (e.g. the North China Plain, the Yangtze River Delta, and the Pearl River Delta) but also central and western China caused by the rapid urbanization and motorization (Kaiser and Qian, 2002). Shortwave radiation at various ground stations in China during the period of 1971–2000 have been going through obvious decreasing trends with the greatest decreases occurring in the central and eastern coastal regions of China (Streets et al., 2008). Che et al. (2007) stated that the horizontal visibility had been significantly decreased in China during 1981–2005, and the increased aerosol loadings were responsible for visibility degradation. Significant anti-correlations between $PM_{2.5}$ concentration and visibility had been revealed in various cities of China, e.g. Beijing (Wang et al., 2006a), Jinan (Yang et al., 2007), Guangzhou (Tao et al., 2009) and Shanghai (Huang et al., 2012b). However, most of the research focused on the relationship between visibility trends and bulk aerosols, rare studies revealed the internal reason of a certain phenomena and gave persuasive explanations.

We choose Shanghai as a typical area to be further explored in this study, as it is the most populous and economically vigorous region in China. Shanghai is located on the eastern tip of the Yangtze River Delta (YRD), which is one of the most industrialized cities with the largest adjacent metropolitan areas in the world. The GDP (Gross Domestic Product) of Shanghai increased five fold in the decade from 1996 to 2006 and the numbers of automobiles increased from 0.47 to 2.53 million during these years (UNEP, 2009). Shanghai has long suffered from visibility impairment as a result of intense industrial and domestic pollutant emissions with high humidity (Huang et al., 2012a, 2012b). During the past decade, especially during the China's 11th Five-Year-Plan, China emphasized on the reduction of SO_2 emission. Also, when the local government prepared for the 2010 Shanghai World Expo, great efforts have been made to reduce emissions in Shanghai (Lin et al., 2013). In this study, the inter-annual variation of visibility and occurrence frequency of haze from 2004 to 2008 in Shanghai is presented. The evolution of the frequency distribution patterns of major pollutants (i.e. SO_2, NO_2 and PM_{10}) is examined to explain the inter-annual trend of visibility. The progression of aerosol chemical species is further investigated to reveal the causes of the visibility decrease and the relationship between visibility degradation and aerosol components. The observational evidences are suggested to design effective control strategies for visibility improvement.

2. Methodology

2.1. Observational site

The observational site (31.3°N, 121.5°E) in this study is on the roof (~20 m) of a teaching building on the campus of Fudan University in Yangpu District of Shanghai. Almost no high buildings were around this sampling site. More than 20 million residents (13 million residents with registered permanent residence plus more than 10 million without permanent residence) are living in this area. This site could be regarded as representative of the megacity, standing for the mixing of emissions from residential, traffic, construction, and industrial sources (Huang et al., 2013).

2.2. Aerosol sampling and chemical analysis

Aerosol samples of TSP and $PM_{2.5}$ were collected on Whatman® 41 cellulose acetate filters (Whatman Inc., Maidstone, UK) using medium-volume samplers manufactured by Beijing Geological Instrument-Dickel Co., Ltd. (model: TSP/PM_{10}/$PM_{2.5}$–2; flow rate: 77.59 l min^{-1}). An inter-comparison study of different types of filters showed that the cellulose acetate filters could quantitatively collect and retain the semi-volatile compounds such as ammonium nitrate aerosol (Schaap et al., 2004). One-month samples were collected in each season from 2004 to 2008: spring (March 15–April 15), summer (July 15–August 15), autumn (October 15–November 15), and winter (December 15–January 15). The duration time of the daily sampling was generally 24 h. More samples with shorter duration time were collected during heavy polluted days. Filters were taken back to the laboratory as soon as each day's sampling was over, and preserved in the refrigerator under a temperature of less than 4 °C to prevent the loss of any aerosol compounds as far as possible. The filters before and after sampling were weighed using an analytical balance (Model: Sartorius 2004MP) with a reading precision of 10 μg after stabilizing under constant temperature (20 ± 1 °C) and humidity (40 ± 1%) in a chamber for 48 h. All the procedures were strictly quality controlled to avoid the possible contamination of samples.

Eleven inorganic ions (SO_4^{2-}, NO_3^-, F^-, Cl^-, NO_2^-, PO_4^{3-}, NH_4^+, Na^+, K^+, Ca^{2+}, and Mg^{2+}) and four organic acids (formic, acetic, oxalic, and methylsulfonic acid (MSA)) were analyzed by Ion Chromatography (ICS 3000, Dionex), which consisted of a separation column (Dionex Ionpac AS 11), a guard column (Dionex Ionpac AG 11), a self-regenerating suppressed conductivity detector (Dionex Ionpac ED50) and a gradient pump (Dionex Ionpac GP50). The detail procedures were given elsewhere (Yuan et al., 2003).

A total of 20 elements (Al, Fe, Mn, Mg, K, Ti, Sc, Na, Sr, Ca, Co, Cr, Ni, Cu, Pb, Zn, Cd, V, S, and As) were analyzed. Half of each sample and blank filter was digested at 170 °C for 4 h in high-pressure Teflon digestion vessel with 3 ml concentrated HNO_3, 1 ml

concentrated HCl, and 1 ml concentrated HF. After cooling, the solutions were dried, and then diluted to 10 ml with distilled deionized water. All elements were measured by using an inductively coupled plasma atomic emission spectroscopy (ICP-OES; SPECTRO, Germany). The detailed analytical procedures were given elsewhere (Zhuang et al., 2001). Black carbon (BC) was analyzed by Smokerstain Reflectometer (UK, Model, M 43D).

2.3. Meteorology data and other data

Meteorological data (including visibility, relative humidity, temperature and wind speed) used in this study are provided by the National Climatic Data Center (NCDC). The Shanghai Hongqiao meteorological station is located southwest, approximately 20 km from the sampling site. Visibility was measured by using a Vaisala LT31 Transmissometer. The LT31 incorporated a white LED, which provided a wide spectrum light source for the best accuracy in transmittance measurement. The visibility measured by using this instrument represented the extinction, i.e. the sum of scattering and absorbing. An extensive automated quality control was applied to correctly 'decode' as much of the synoptic data as possible and to eliminate random errors found in the original data (Lott, 2004; Smith et al., 2011). Raw data are originally archived using Coordinated Universal Time (UTC) and the time was converted to local time (UTC+8) to coordinate with the time of measurement. The visibility in Hongqiao Station was recorded up to a threshold of 11.3 km due to the practice of not reporting visibilities greater than certain distances in most stations of China. To avoid the impact of the 'cluster' value of the threshold value of the instrument used for the measurement of visibility, the median value of the hourly visibility during a day was used in this study. Specific weather events such as rain, snow, and typhoon were excluded from the data analysis.

The daily air quality data (SO_2, NO_2, and PM_{10}) in Shanghai were reported from Shanghai Environmental Monitoring Center (SEMC). The data were average values from 10 monitoring stations located in different places of Shanghai.

2.4. Reconstruction of light extinction

In this study, the total light extinction coefficient is estimated using the IMPROVE algorithm as follows:

$$\begin{aligned} b_{\mathrm{ext}}\left(\mathrm{M\ m^{-1}}\right) = {} & 3.0 \times f(\mathrm{RH}) \times \left\{\left[(\mathrm{NH_4})_2\mathrm{SO_4}\right] + \left[\mathrm{NH_4NO_3}\right]\right\} \\ & + 4.0 \times [\mathrm{Organics}] + 10.0 \times [\mathrm{BC}] + 1.0 \\ & \times [\mathrm{fine-dust}] + 0.6 \times [\mathrm{coarse-dust}] \\ & + \mathrm{Rayleigh\ \ Scattering(site\ \ specific)}, \end{aligned}$$

The numbers in the front of each species were the mass extinction efficiency ($m^2\ g^{-1}$) for each species. f(RH) denotes the hygroscopic growth factor, which determines the variability in b_{ext} caused by the relative humidity. In the estimation, only ammonium sulfate and ammonium nitrate were considered to be hygroscopic. f(RH) was obtained from a look-up table given in Malm et al. (1994). Daily f(RH) values are averaged from the hourly f(RH) values of each sampling day. The Rayleigh scattering was negligible compared to the aerosol extinction and thus is ignored in this study. To verify the reliability of this reconstructed extinction, the optical light extinction estimated from Koschmieder equation was used for comparison.

$$b_{\mathrm{ext}}\left(\mathrm{M\ m^{-1}}\right) = 3.912/\mathrm{Vis}$$

3. Results and discussion

3.1. Inter-annual, seasonal variation of visibility and haze frequency during 2004–2008

Fig. 1 plots the average horizontal visibility during 2004–2008 from 388 NCDC stations in China. Generally, the spatial distribution of visibility resembled the population density of China, indicating the significant impact of human activities on the visibility impairment. Low visibility regions (less than 20 km) distributed in widespread areas of China, stretching from northeastern China, the North China Plain, Eastern China, Sichuan Basin to Southern China. Among those areas, the occurrences of haze (visibility less than 10 km) were mainly observed over the areas of Beijing–Tianjin–Hebei, the Yangtze River Delta, part of Central China, the Sichuan Basin, and the Pearl River Delta region. In the discussions below, we will focus on a megacity, Shanghai in the Yangtze River Delta region, to investigate the major factors contributing to the heavy haze in this region.

Fig. 2 depicts the inter-annual trend of visibility on a seasonal basis from 2004 to 2008 in Shanghai. The seasonal average visibility in spring, summer, autumn, and winter was 7.7 km, 8.4 km, 8.1 km, and 6.5 km, respectively. This clearly indicates that visibilities in Shanghai had significantly exceeded the haze criteria of 10 km throughout all four seasons with severe air quality problems. We grouped all days into two categories, i.e., haze days (Vis $\leq$ 10 km) and normal days (Vis $>$ 10 km) based on the daily median visibility. The average number of haze days in winter reached 55 days (88% of non-precipitation days), which was close to that of 89% in spring and higher than that of 61% in summer and 65% in autumn. The cold seasons evidently showed extremely high frequencies of haze. Fig. 2 also shows the number of haze days and the inter-annual trends of visibility and haze frequency from 2004 to 2008. It is found that the seasonal number of haze days and the frequency of haze fluctuated between years but with almost no discernible trends, thus resulting in insignificant annual trends of visibility.

To explain the behavior of multi-year visibility, the inter-annual variations of major meteorological parameters and air pollutants were first investigated by using the Duncan's multiple range test. As shown in Table S1, meteorological (temperature, dew point, atmospheric pressure, and wind speed) conditions showed no obvious differences during 2004–2008 on the 95% significant level. While for the pollutants gases, SO_2 showed significant differences among years (except for 2006 and 2008) and NO_2 also showed differences

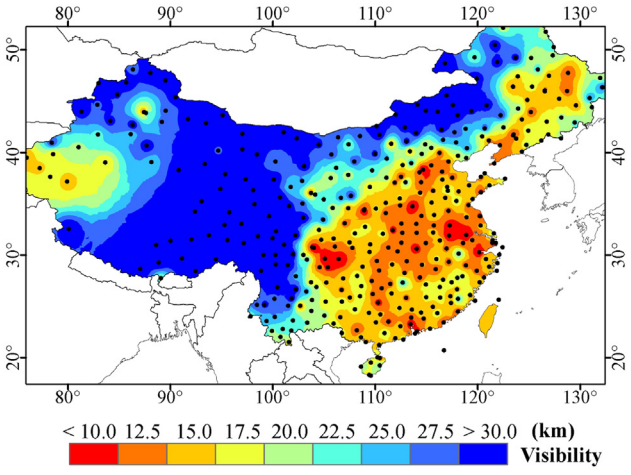

Fig. 1. Spatial distribution of average horizontal visibilities during 2004–2008 from 388 NCDC stations in China. Black dots represent the locations of the available NCDC stations during the study period.

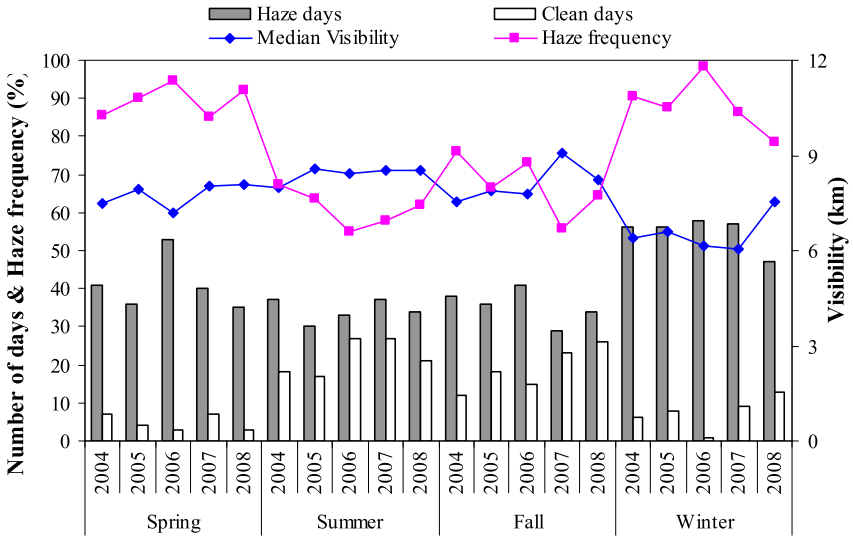

Fig. 2. The number of clean days (visibility > 10 km) and haze days (visibility ≤ 10 km), the mean visibility and haze frequency of four seasons during 2004–2008 in Shanghai. Rain, fog, and snow days are excluded for the analysis.

between 2004–2005 and 2006–2008. However, no significant difference of the inter-annual variations of PM_{10} (except for 2004) was observed. Fig. 3 further illustrates the frequency distribution of SO_2, NO_2, and PM_{10} concentrations at fixed concentration bins in each year from 2004 to 2008. As illustrated in Fig. 3a, the frequency distribution pattern of SO_2 changed rapidly for these years. It tended to skew towards lower concentrations year by year as well as less occurrences of high level SO_2 days. SO_2 centered at around 40 μg/m^3 in 2008, about 10 μg/m^3 lower than previous years. This was mainly attributed to the cessation in operation of some inefficient units in local coal-fired power plants, and also the widespread installation of the Flue-Gas Desulphurization (FGD) in Shanghai in recent years (UNEP, 2009). A similar shifting trend of NO_2 was also observed. In 2004 and 2005, most occurrences of NO_2 concentrations were found in a wide range of around 40–80 μg/m^3. While in 2006 and 2007, the distribution of NO_2 narrowed and mainly centered around 60 μg/m^3. Also, the occurrence frequency of relatively high NO_2 events was reduced as compared to the previous years. In 2008, NO_2 had an evident shift to peak at around 40 μg/m^3. The annual changing trend of the frequency distribution of NO_2 was not as strong as for SO_2. Two major reasons are theorized for this trend. First, the efficiency of the Selective Non-catalytic Reduction (SCR) technology on NO_x emission reduction (~40%) in power plants was much lower than that of FGD (>90%), and the application of this technology was far less widespread than FGD. Further, the rapid growth of the number of vehicles (mainly private vehicles) and the total miles traveled in Shanghai was believed to be another contributory cause of the relatively high NO_2 concentrations. Compared to SO_2 and NO_2, the distribution pattern of PM_{10} varied less strongly with a slight shift towards lower PM_{10} concentrations in recent years. For instance, the high occurrence frequency of PM_{10} mainly centered in the range of 60–80 μg/m^3 with more than 25% of days with PM_{10} higher than 100 μg/m^3 in 2004. While in 2005–2007, the distribution pattern of PM_{10} extended to center in the range of 40–100 μg/m^3 with around 20% of days higher than 100 μg/m^3. In 2008, the distribution pattern became sharper and more centralized at around 70 μg/m^3, and the percentage of days with PM_{10} higher than 100 μg/m^3 dropped to less than 10%. Overall, it was found that although the concentrations of SO_2 and NO_2 had decreases, the aerosol concentration in Shanghai was not obviously improved. This implies that some other pollutant species could have compensated the effects of the mitigated SO_2 and NO_2 emissions. As aerosol was the major contributor to atmospheric visibility, visibility was hence not obviously improved as shown in Fig. 2. In the following sections, factors contributing to visibility impairment and controlling the variation of visibility will be discussed.

3.2. Comparison of meteorological conditions and aerosol species under different haze conditions

A grouping method was used to qualitatively study factors affecting visibility using the multi-year dataset from 2004 to 2008. All sampling days with available aerosol chemistry measurement were categorized into three groups, i.e. the normal days (abbreviated as ND, Vis > 10 km), moderate haze days (abbreviated as MH, 5 km < Vis ≤ 10 km), and heavy haze days (abbreviated as HH, Vis ≤ 5 km). Mean values of meteorological parameters (temperature, wind speed, and relative humidity) and aerosol (with chemical components) concentrations were compared according to these three groups. The measured chemical components were grouped into four categories, i.e., total water soluble ions (TWSI), mineral aerosol, black carbon (BC), and the rest assumed to be organics. TWSI was calculated by summing all the measured inorganic ions. Mineral aerosol was estimated by summing the major mineral elements with oxygen for their normal oxides using the formula [Mineral aerosol] = 2.2[Al] + 2.49[Si] + 1.63[Ca] + 2.42[Fe] + 1.94[Ti] (Malm et al., 1994). Table 1 list the mean value and standard deviation of each parameter. In addition, we calculated the "*R*" ratio, which is defined as the average of each parameter in each of the three groups divided by the average of each parameter in the whole samples. This ratio can be used to qualitatively assess what factors are more associated with the haze formation. As for the three meteorological parameters, the "*R*" ratio of temperature and wind speed both showed large variances with the sequence of ND > MH > HH, indicating that the haze formation was more favored under lower temperature and lower wind speed. Lower temperature was a result of less solar insolation which could induce lower mixing layer heights. Hence, the severe haze preferentially occurred in the cold seasons when temperature was lower. Lower wind speed did not facilitate the dispersion of air pollution, increasing the possibility of haze formation. The "*R*" ratio of the hygroscopic growth factor *f*(RH) followed an opposite sequence of HH > MH > ND, suggesting the haze formation was more favored under higher humidity due to the fast growth of hygroscopic chemical species in aerosol.

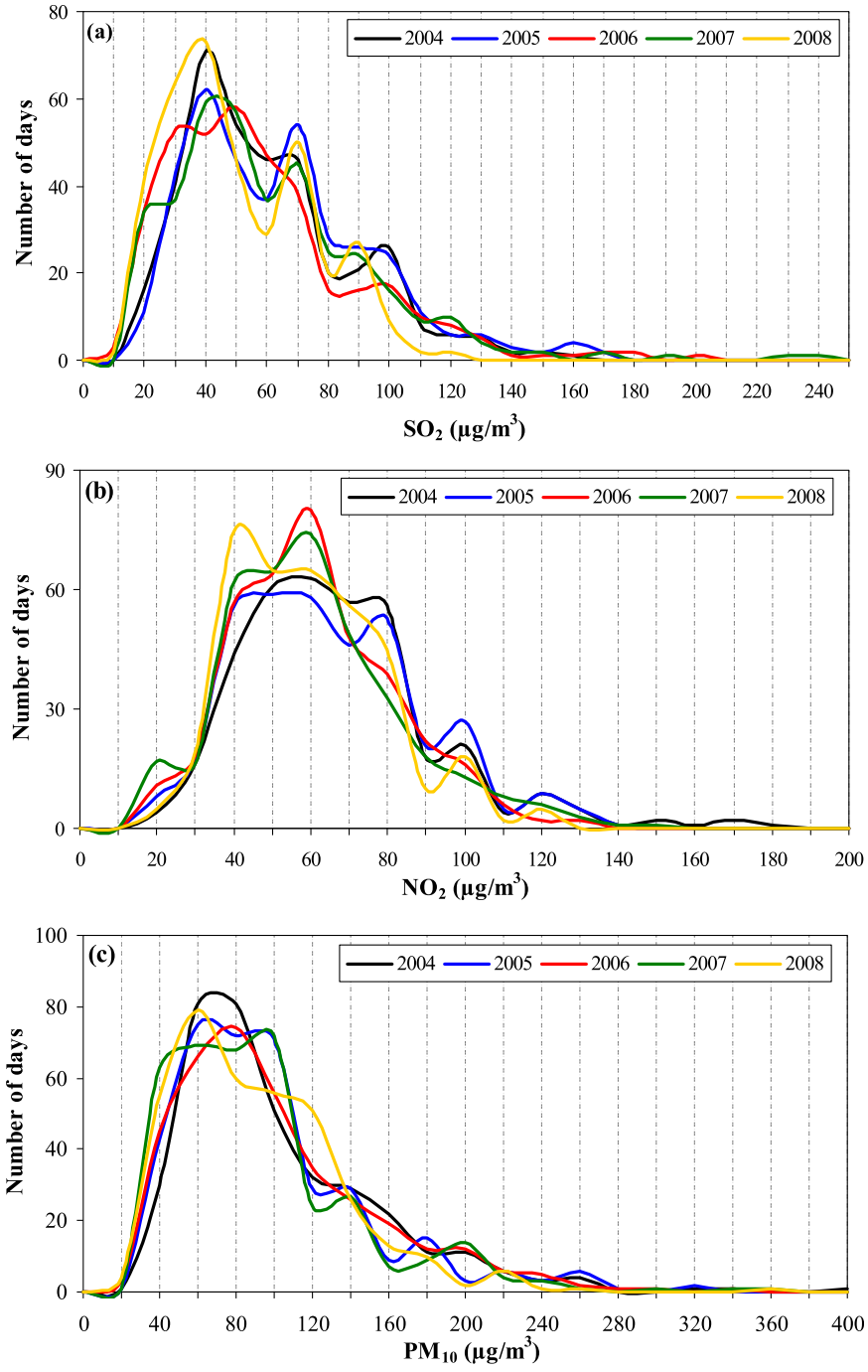

Fig. 3. The annual variation of frequency distributions of SO_2, NO_2 and PM_{10} concentration in Shanghai during 2004–2008.

As for the chemical species, the "*R*" ratio of TWSI presented the largest differences among the various species under normal days, moderate haze and heavy haze with values of 0.76, 1.03, and 1.51, respectively. The soluble ions were elevated more than 50% in the heavy haze as compared to its average of all collected samples. BC also had similar variation as TWSI although its variation was not as pervasive as that of TWSI. For instance, the mean BC concentration under the heavy haze was 29% higher than its average of the all samples. However, we did not observe distinct differences of the "*R*" ratio of minerals under the three groups, indicating the mineral aerosol negligibly contributed to the haze formation. The "*R*" ratios of almost all the ions demonstrated increasing tendencies from the normal day group to the heavy haze group. Of which, NO_3^-, SO_4^{2-}, NH_4^+, K^+, and $C_2O_4^{2-}$ showed the most robust differentiations. NO_3^- and SO_4^{2-} were the most abundant species among the soluble ions as shown in Table 1, and mainly formed from fossil fuel combustion. This indicated that anthropogenic emissions were always the major contributors to haze formation. It should be noted that oxalate ($C_2O_4^{2-}$), as one of the organic acid ions, had a very significant increase during heavy haze events. Oxalate could be derived from various sources such as biogenic emission or biomass burning. Although the concentration of organic aerosol was not measured in this study, we assume that the water soluble organic aerosol, as represented by $C_2O_4^{2-}$, should also contribute to the haze formation. Apart from the species as referred above, other ions such as NH_4^+ and K^+ also had moderate differences among the three groups. As the

Table 1
The mean value (with one standard deviation) of major meteorological parameters and aerosol chemical species in both $PM_{2.5}$ and TSP during 2004–2008. The "*R*" and "R_2" ratios (see footnote) are also calculated.

Parameters		Total samples		[b]The "*R*" ratio			[c]The "R_2" ratio
		Mean	S.D.	Vis > 10	5 < Vis ≤ 10	Vis ≤ 5	
Meteorology	Vis (km)	7.77	3.04	1.33	0.87	0.47	−0.65
	Temp (°C)	16.94	9.47	1.04	0.97	0.88	−0.16
	WS (m s^{-1})	3.48	1.47	1.17	0.95	0.71	−0.39
	[a]*f*(RH)	3.02	1.14	0.90	1.06	1.15	0.28
$PM_{2.5}$ species (μg/m^3)	$PM_{2.5}$	60.62	39.67	0.86	1.02	1.43	0.66
	TWSII	19.78	12.57	0.76	1.03	1.51	0.99
	BC	2.39	1.63	0.83	1.02	1.29	0.55
	Mineral	16.20	25.18	1.08	0.96	1.33	0.24
	Others	22.24	16.27	0.90	0.94	1.29	0.44
	Na^+	0.54	0.39	1.03	1.10	0.96	−0.07
	NH_4^+	3.30	2.29	0.73	1.17	1.39	0.89
	K^+	0.61	0.52	0.71	1.01	1.46	1.04
	Mg^{2+}	0.13	0.14	0.98	1.03	1.22	0.24
	Ca^{2+}	0.94	1.10	1.03	1.09	1.28	0.24
	NO_3^-	4.10	4.02	0.70	0.95	1.77	1.51
	SO_4^{2-}	7.01	5.51	0.70	0.97	1.62	1.31
	$C_2O_4^{2-}$	0.13	0.75	0.85	1.00	2.17	1.54
	Cl^-	1.62	1.49	0.94	0.95	1.34	0.42
	F^-	0.13	0.21	1.01	1.25	1.14	0.13
	NO_2^-	0.23	0.39	0.87	1.09	1.09	0.24

[a] *f*(RH): hygroscopic growth factor (unitless).
[b] The ratios of the mean values of all the parameters under three visibility groups (i.e. Vis > 10, 5 < Vis ≤ 10, and Vis ≤ 5) versus the mean values of all samples.
[c] $R_2 = R(\text{Vis} \le 5)/R(\text{Vis} > 10) - 1$.

major neutralization cation for the acids, the role of NH_4^+ in haze formation was expected. K^+ is a typical tracer for biomass burning (Andreae, 1983). Its behavior indicated that biomass burning was also one of the source contributors to haze formation. Shanghai, located in the Yangtze River Delta region, is one of the most important agricultural bases in China. Biomass burning has been investigated as one of the three typical haze types in Eastern China, especially during harvest seasons (Huang et al., 2012a). Some other ions, e.g. Ca^{2+}, Mg^{2+}, and Cl^-, had smaller variations among the three groups, indicating their roles in haze formation were less important. Compared to most of the ions, the only exception was Na^+, whose "*R*" ratio showed an opposite tendency of decreasing from the normal day group to the heavy haze group. Na^+ was mainly derived from the marine source, as Shanghai is a coastal city (Huang et al., 2008). Higher Na^+ concentrations suggested greater possibilities of air masses from an oceanic source, which transported relatively clean air flows and thus improved visibility. This effect was more prominent in TSP, as Na^+ mainly accumulated in the coarse mode (Table S2).

Reconstruction of light extinction by using aerosol chemical components could further corroborate the analysis above. Fig. 4a compares the light extinction estimated by the aerosol chemical components and by visibility as described in Section 2.4. The regression slope is 0.94, very close to the 1:1 line, indicating the extinction budgets could be reasonably estimated. Fig. 4b apportions the average contributions of major aerosol chemical components to the total light extinction. TWSI ranked the biggest contributor to the light extinction, with SO_4^{2-}, NO_3^-, and NH_4^+ accounting for 23%, 13%, and 11%, respectively. The estimated organic matter also contributed significantly of 37%. Although BC only constituted 2–4% of the aerosol mass, its contribution to light extinction reached 11% due to its strong absorbing efficiency. Dust showed a less contribution of ~5% among the aerosol components.

The aerosol species in TSP generally showed similar behaviors as in $PM_{2.5}$ (Table S2). Compared to $PM_{2.5}$, the "*R*" ratios of TSP had smaller divergences among the three groups, especially for those ions with abundant concentrations. This was expected as coarse particles had lower extinction efficiency to sunlight. Overall, we found that the "*R*" ratios of most parameters were close to 1.00 under the moderate haze group, which implied that the moderate

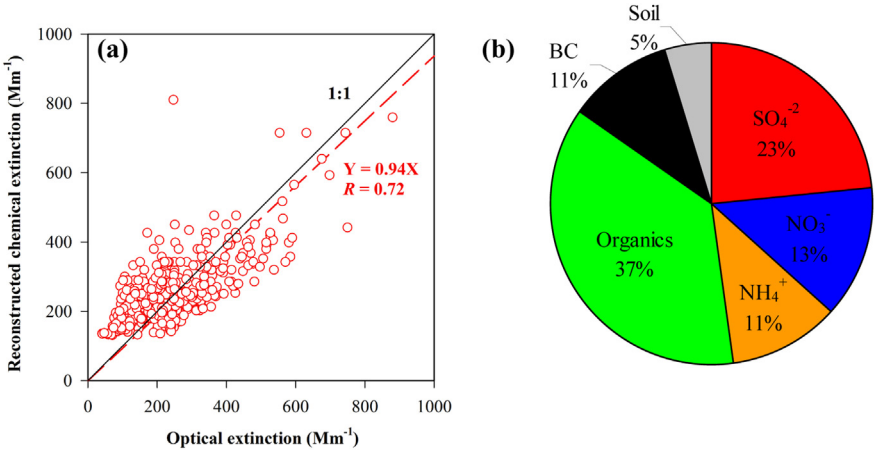

Fig. 4. (a) Correlation between the light extinction estimated by the aerosol chemical components and that estimated by measured visibility (b) average contributions of major aerosol chemical components to the total light extinction.

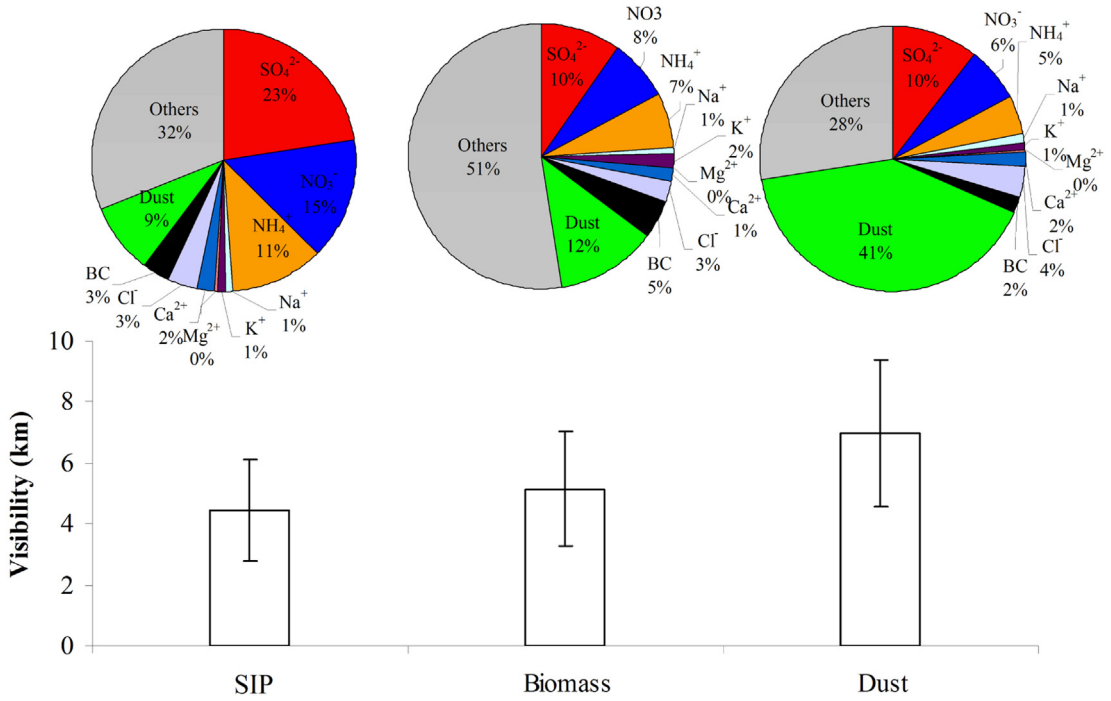

Fig. 5. Average contribution of aerosol chemical compositions to $PM_{2.5}$ under three types of haze (i.e. secondary inorganic pollution (SIP), biomass and dust) identified during 2004–2008 (top pie charts). The average visibility (with one standard deviation) under the three haze types is shown in the bottom bar charts.

haze (5 km $<$ Vis $\leq$ 10 km) condition has become standard and normal for present-day of Shanghai.

3.3. *Visibility impairment under different haze types*

Huang et al. (2012a) categorized the frequent occurrences of haze over Eastern China into three major types, i.e. secondary inorganic pollution, dust, and biomass burning. In this study, we also grouped all haze days during 2004–2008 into these three types. To identify a high air pollution event to be dominantly caused by dust, several criteria need to be satisfied. These criteria are that the ratio of $PM_{2.5}$ in TSP should be below 0.5; the concentration of elemental Al should be significantly higher than background; and the backward trajectories should point to a desert source area, e.g. the Gobi or Taklamakan Deserts. Finally, all dust events are to be verified by the "Sand-dust Weather Almanac (China)" book annually published by the China Meteorological Administration. To identify haze events to be dominantly caused by biomass burning, K^+ is utilized as a typical tracer. By regarding the seasonal average level of K^+ in Shanghai (see Table 3 in Wang et al., 2006b) as a baseline, those days with K^+ concentrations higher than this baseline in each season were first identified. Then, the daily fire spot maps from the MOD14 products retrieved from MODIS (Moderate-Resolution Imaging Spectroradiometer) were further used to verify whether there were fires occurring around the Yangtze River Delta region or not. After excluding the dust and biomass burning events, the remaining days were further identified to be the haze events caused by secondary inorganic pollution. It is assumed that if the ratio of the extinction contributed from the total secondary inorganic aerosol in the total extinction exceeded 50%, then we think the haze day was dominated by the secondary inorganic pollution. By using this threshold, the haze events caused by dominated organic aerosol could be possibly excluded.

The percentage contributions of various chemical components to $PM_{2.5}$ under the three haze types as defined above are shown in Fig. 5. Comparisons of aerosol chemistry among the three groups demonstrated that inorganic soluble ions contributed the most to $PM_{2.5}$ (57%) under the haze type of secondary inorganic pollution while least under dust (29%). In the category of haze caused by biomass burning, the unmeasured part (labeled as "Others" in Fig. 5) contributed an average of more than 50% to $PM_{2.5}$. We assume this unmeasured part should be mainly composed of organic aerosol as a major product during biomass burning. In the category of haze caused by long-range transported dust, the mineral aerosol was expected to dominate the aerosol components with a mass fraction of 41%. The average visibilities under the three haze groups are also shown in Fig. 5. Under haze events caused by secondary inorganic pollution, the mean visibility reached the lowest value of 4.52 ± 1.78 km, followed by the biomass burning haze group of 5.15 ± 1.87 km, while the dust group showed relatively high visibility of 6.98 ± 2.38 km. The contribution of black carbon, which is the most efficient light extinction aerosol component, did not vary significantly among the three haze groups. Since it constituted only a minor part in $PM_{2.5}$, the level of soluble ions and organic aerosol would determine the magnitude of visibility due to their strong light extinction efficiencies. Under those haze events caused mainly by secondary inorganic pollution, soluble ions were the major aerosol components affecting visibility as it becomes more hygroscopic under relatively high humidity and further impairs visibility. For those haze events caused by biomass burning, although organic aerosol was also a strong light extinction species, its lower hygroscopicity than the inorganic ions may result in relatively weaker light extinction. Thus, the mean visibility caused by biomass burning was higher than that from the secondary inorganic pollution. Compared to inorganic soluble ions and organic aerosol, mineral aerosol had much weaker light extinction efficiency, thus, the visibility caused by dust invasion was not necessarily low even though the particle concentrations during dust events were usually much higher than that under other circumstances.

Among all the identified haze days during 2004–2008, the haze caused by secondary inorganic pollution dominated with the frequency of 64%, while the frequencies of biomass burning and dust

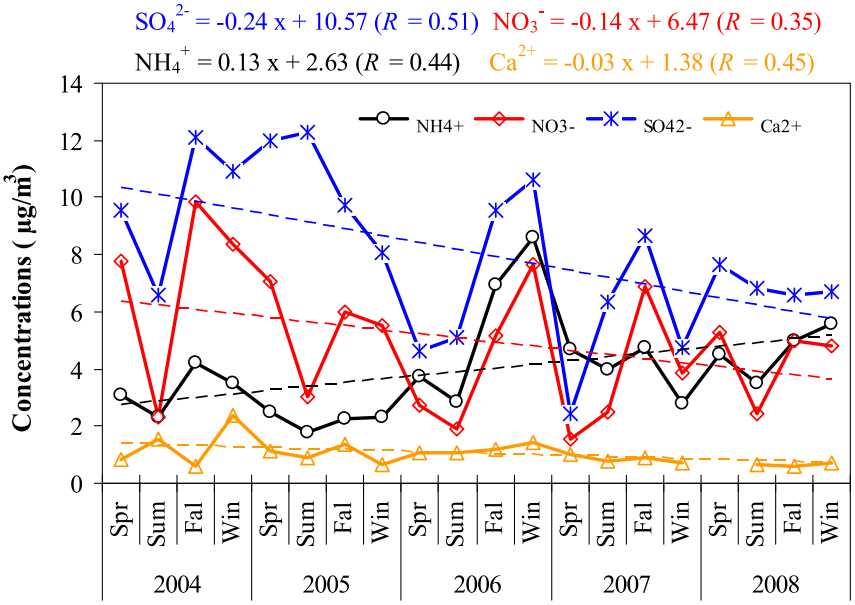

Fig. 6. The inter-annual trends of SO_4^{2-}, NO_3^-, NH_4^+ and Ca^{2+} during 2004–2008 on a seasonal basis. The linear regression equations with correlation coefficients are shown on top of the figure.

were 25% and 11%, respectively. The precursors of secondary inorganic pollutions were mainly from anthropogenic sources, such as SO_2, NO_x, and NH_3 emissions, which were the major emitted pollutants over the urban areas throughout the whole year. Since biomass burning and dust were both episodic events (i.e. occurred in harvest season and spring dry season, respectively), their impacts on the occurrence of haze events should be far less than that of anthropogenic emissions. Controlling anthropogenic emissions is the most efficient way to improve air quality and visibility in the vicinity of the study area.

3.4. Factors controlling the inter-annual variation of visibility

The inter-annual visibilities of Shanghai had negligible trends (regression slope = 0.02, correlation coefficient $r = 0.17$) from 2004 to 2008 (see Section 3.1), although the concentrations of SO_2 and NO_2 tended to shift to lower values based on the frequency distribution of the two pollutant precursors (Fig. 3). To explain this "inconsistence", the inter-annual variations of the major aerosol acid ions (SO_4^{2-} and NO_3^-) and neutralizers (NH_4^+ and Ca^{2+}) in $PM_{2.5}$ from 2004 to 2008 are plotted based on a seasonal basis in Fig. 6. Decreasing trends of sulfate and nitrate were observed with moderate correlation coefficients of 0.51 and 0.35, respectively. The annual decreasing rates of SO_4^{2-} and NO_3^- concentrations reached 0.96 and 0.56 μg/m^3/yr, respectively. SO_4^{2-} had a greater decreasing trend than that of NO_3^-, with the reason explained in Section 3.1. The decreasing trends of SO_4^{2-} and NO_3^- were consistent with the decreasing trend of SO_2 emission of Shanghai (Shanghai Statistical Yearbook, 2013) and that of NO_x emissions estimated from satellite (Gu et al., 2013). On the contrary, a significant increasing trend of NH_4^+ was clearly observed with the correlation coefficient of 0.44. The annual increasing rate of NH_4^+ concentrations reached 0.52 μg/m^3/yr. Ammonia served as the principal base which neutralized acids such as H_2SO_4 and HNO_3 when they condensed onto particles. The increase of NH_4^+ induced the shift from Ca^{2+} to NH_4^+ neutralization, which would change the optical properties and reinforce the extinction efficiency of the aerosol in Shanghai.

The reason for the increased ammonium could be elucidated from the comparison between the equivalent concentrations (μeq/m^3) of $[NH_4^+]$ vs. $[SO_4^{2-} + NO_3^-]$ and $[NH_4^+ + Ca^{2+}]$ vs. $[SO_4^{2-} + NO_3^-]$ in each year during 2004–2008 (Fig. 7). The cations and anions had significant correlations with each other, indicating that NH_4^+ and Ca^{2+} both played important roles in the process of acid neutralization. Via the slopes (forced through zero) of $[NH_4^+]$ vs. $[SO_4^{2-} + NO_3^-]$ and $[NH_4^+ + Ca^{2+}]$ vs. $[SO_4^{2-} + NO_3^-]$, the relative role of NH_4^+ and Ca^{2+} on the formation of sulfate and nitrate salts could be quantitatively assessed by using the formula below.

$$NF\left(NH_4^+\right) = Slp\left(\frac{\left[NH_4^+\right]}{\left[SO_4^{2-} + NO_3^-\right]}\right)$$

$$NF(Ca^{2+}) \begin{cases} = Slp\left(\frac{\left[NH_4^+\right] + \left[Ca^{2+}\right]}{SO_4^{2-} + NO_3^-}\right) - Slp\left(\frac{\left[NH_4^+\right]}{SO_4^{2-} + NO_3^-}\right), & \text{if } Slp\left(\frac{\left[NH_4^+\right] + \left[Ca^{2+}\right]}{\left[SO_2^{2-} + NO_3^-\right]}\right) \le 1.0 \\ = 1.0 - Slp\left(\frac{\left[NH_4^+\right]}{SO_4^{2-} + NO_3^-}\right), & \text{if } Slp\left(\frac{\left[NH_4^+\right] + \left[Ca^{2+}\right]}{SO_4^{2-} + NO_3^-}\right) > 1.0 \end{cases}$$

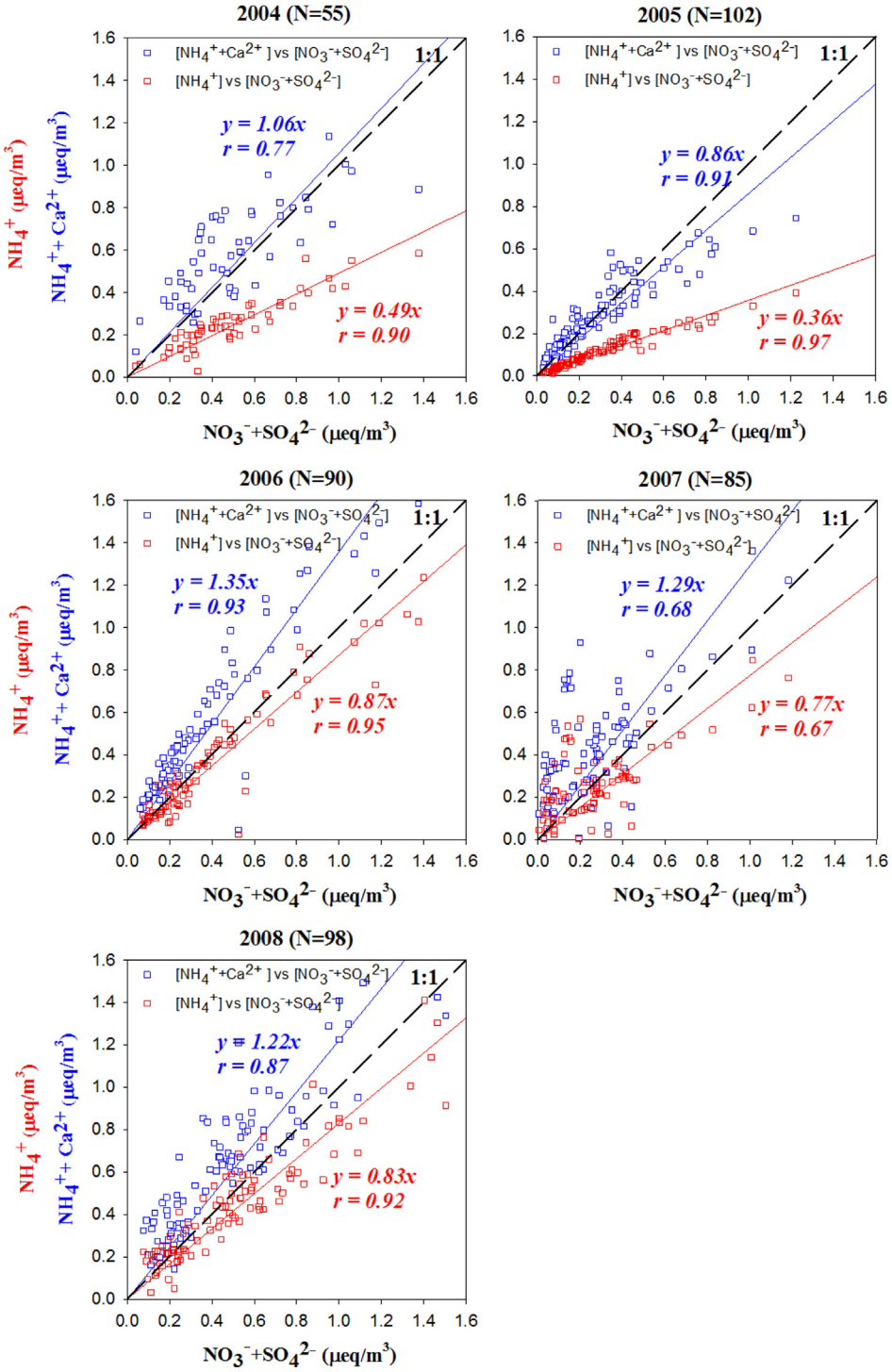

Fig. 7. Linear correlations between NH_4^+ and $[SO_4^{2-} + NO_3^-]$ and that between $[NH_4^+ + Ca^{2+}]$ and $[SO_4^{2-} + NO_3^-]$ from 2004 to 2008. All units are shown in equivalent concentrations (μeq/m^3). Linear regressions are forced through zero with regression equations and correlation coefficients indicated in the figure. The 1:1 dashed lines are also shown.

For this demonstration, *NF* and *Slp* represent the neutralization fraction and the regression slope (shown in Fig. 7), respectively. On an annual basis, the two regression slopes presented much larger gaps (the difference of the two slopes) in the early years. For example, the gap reached 0.51 and 0.50 in 2004 and 2005, respectively. The neutralization fraction of NH_4^+ and Ca^{2+} on the total acids was 0.49 and 0.51 in 2004, respectively, and it was 0.36 and 0.50 in 2005, respectively. Thus, the roles of NH_4^+ and Ca^{2+} on the acid neutralization were close to each other in these two years. From 2006 to 2008, the gaps between the two regression slopes were evidently narrowed, indicating that Ca^{2+} was playing a less important role from 2006 to 2008. The neutralization fraction of Ca^{2+} on the total acids had decreased to 0.13, 0.23, and 0.17 during 2006–2008, respectively. Hence, the neutralization fraction of NH_4^+ on the total acids was elevated to around 80% in the last three years as compared to that of 50% in the first two

years. The decreasing trend of Ca^{2+} (Fig. 6) was the major cause for this transition of chemical species in aerosol. Construction work and roadside dust in Shanghai contributed to the major sources of Ca^{2+} (Huang et al., 2013; Wang et al., 2006b). On the occasion of preparation for the 2010 World Expo held in Shanghai, the local government implemented various control measures on emissions. Of which, emission control on construction works and roadside dust was a major measure for reducing the primary emission, including the establishment of a dust control zone from downtown Shanghai to suburban areas. In addition, requirements were implemented for the covering or containment of idle soil, cement, and construction waste and frequent cleanup of main traffic roads. Thus, the role of Ca^{2+} on acid neutralization decreased due to its emission reduction. In addition, the emission of NH_3 in Shanghai and some adjacent areas was slightly insufficient (Wang et al., 2011). This resulted in the replacement of $CaSO_4$ and $Ca(NO_3)_2$ by the enhanced formation of $(NH_4)_2SO_4$ and NH_4NO_3 in particles. Since the ammoniated sulfate and nitrate predominantly accumulated in the fine mode of aerosol, they were more efficient at scattering light than those neutralized by the alkaline minerals, which predominantly accumulated in the coarse mode. In addition, the ammonium salts were more hygroscopic than the calcium salts. Thus, the shift from Ca^{2+} to NH_4^+ neutralization resulted in stronger light extinction. Overall, the replacement of calcium salts by ammonium salts should be the major cause for the negligible improvement of visibility in Shanghai in this study period. A multi-pollutant control strategy to reduce both acid (e.g. SO_2 and NO_x) and alkaline (e.g. NH_3) precursors should be an effective and sound way to reduce the level of particulate matters. The NH_3 emission was dominated by agricultural sources, notably animal manure and fertilizer application. The Yangtze River Delta, where Shanghai is located, is a traditional agricultural base of China with significant NH_3 hotspots (Huang et al., 2011; Zhao et al., 2012). Currently, there is no environmental protocol set for NH_3 standards in China. The dramatic increase of NH_3 since the late 1970s (Cui et al., 2013) may make China's goal to improve air quality a great challenge.

4. Conclusions

In this study, we conducted a multi-year (2004–2008) analysis of the visibility trend/haze frequency in Shanghai as well as major factors controlling the inter-annual variations of visibility. The major findings are as follows:

1. The seasonal average visibility in spring, summer, autumn, and winter was 7.7 km, 8.4 km, 8.1 km, and 6.5 km, respectively, significantly exceeding the haze criteria of 10 km throughout all four seasons. The frequency distributions of SO_2, NO_2 and PM_{10} indicated that SO_2 and NO_2 both tended to skew towards lower concentrations but not significant for PM_{10}. However, the annual mean visibility in Shanghai was not obviously improved.
2. By using a grouping method, all the study days were categorized into three groups, i.e. normal days, moderate haze days ($5\ km < Vis \leq 10\ km$), and heavy haze days ($Vis \leq 5\ km$). Major meteorological parameters and chemical species were compared under the three groups. The formation of haze was more favored under lower temperature, slower wind speed, and higher relative humidity. Of the aerosol chemical species, soluble ions (NO^-_3, SO_4^{2-}, NH_4^+, K^+, and $C_2O_4^{2-}$) and black carbon were the major contributors to haze, but not for mineral aerosol. It was found that nearly all parameters under the moderate haze group were very close to their mean average for all study days, indicating visibility in the range of 5–10 km had become the "normal" weather in Shanghai.
3. Based on various aerosol chemical tracers and supplementary information, all haze days were grouped into three types, i.e. secondary inorganic pollution, biomass burning, and dust. Comparisons among the three haze types indicated haze caused by the secondary inorganic pollution was associated with lower visibility than the other two, suggesting the importance of controlling anthropogenic emission sources.
4. SO_4^{2-} and NO_3^- both exhibited significant decreasing trends due to strict controls on SO_2 and NO_x emissions in recent years. Oppositely, NH_4^+ showed a significant increasing trend. In comparison between the linear correlations of $[NH_4^+]$ vs. $[SO_4^{2-} + NO_3^-]$ and $[NH_4^+ + Ca^{2+}]$ vs. $[SO_4^{2-} + NO_3^-]$, the role of NH_4^+ and Ca^{2+} on the acids neutralization could be quantitatively evaluated on an annual basis. The two cations almost had equivalent contributions to the formation of sulfate and nitrate in 2004–2005, while the role of Ca^{2+} had tremendously dropped to less than 23% in 2006–2008. Intense control measures on the emission of construction work and roadside dust accounted for the evident decreasing trend of annual Ca^{2+} concentrations. This study determined that the gradual replacement of $CaSO_4$ and $Ca(NO_3)_2$ by $(NH_4)_2SO_4$ and NH_4NO_3 in aerosol should be the major cause of negligible improvement of visibility across Shanghai.

Acknowledgment

This work was supported by National Natural Science Foundation of China [Grant Nos. 41128005 (fund for collaboration with oversea scholars), 21277030], and the great international collaboration project of MOST, China (2010DFA92230). We thank the National Climatic Data Center for providing the meteorological data used in this study. We appreciate Mr. Bill Moore for polishing the language of this paper and we greatly thank two anonymous reviewers for helpful comments and suggestions on improving the manuscript.

Appendix A. Supplementary data

Supplementary data related to this article can be found at http://dx.doi.org/10.1016/j.atmosenv.2014.04.007.

References

Andreae, M.O., 1983. Soot carbon and excess fine potassium: long-range transport of combustion-derived aerosols. Science 220, 1148–1151.
Cass, G.R., 1979. On the relationship between sulfate air quality and visibility with examples in Los Angeles. Atmospheric Environment 13, 1069–1084.
Chameides, W.L., Yu, H., Liu, S.C., Bergin, M., Zhou, X., Mearns, L., Wang, G., Kiang, C.S., Saylor, R.D., Luo, C., Huang, Y., Steiner, A., Giorgi, F., 1999. Case study of the effects of atmospheric aerosols and regional haze on agriculture: an opportunity to enhance crop yields in China through emission controls? Proceedings of the National Academy of Sciences of the United States of America 96, 13626–13633.
Che, H., Zhang, X., Li, Y., Zhou, Z., Qu, J.J., 2007. Horizontal visibility trends in China 1981–2005. Geophysical Research Letters 34, L24706. http://dx.doi.org/10.1029/2007gl031450.
Chen, L.W.A., Chow, J.C., Doddridge, B.G., Dickerson, R.R., Ryan, W.F., Mueller, P.K., 2003. Analysis of a summertime PM2.5 and haze episode in the mid-Atlantic region. Journal of the Air & Waste Management Association 53 (8), 946–956.
Cui, S., Shi, Y., Groffman, P.M., Schlesinger, W.H., Zhu, Y.G., 2013. Centennial-scale analysis of the creation and fate of reactive nitrogen in China (1910–2010). Proceedings of the National Academy of Sciences of the United States of America. http://dx.doi.org/10.1073/pnas.1221638110.
Gu, D.S., Wang, Y.H., Smeltzer, C., Liu, Z., 2013. Reduction in NO_x emission trends over China: regional and seasonal variations. Environmental Science & Technology 47, 12912–12919. http://dx.doi.org/10.1021/Es401727e.
Hsu, N.C., Gautam, R., Sayer, A.M., Bettenhausen, C., Li, C., Jeong, M.J., Tsay, S.C., Holben, B.N., 2012. Global and regional trends of aerosol optical depth over land and ocean using SeaWiFS measurements from 1997 to 2010. Atmospheric Chemistry and Physics 12, 8037–8053. http://dx.doi.org/10.5194/acp-8012-8037-2012.

Huang, C., Chen, C.H., Li, L., Cheng, Z., Wang, H.L., Huang, H.Y., Streets, D.G., Wang, Y.J., Zhang, G.F., Chen, Y.R., 2011. Emission inventory of anthropogenic air pollutants and VOC species in the Yangtze River Delta region, China. Atmospheric Chemistry and Physics 11, 4105–4120. http://dx.doi.org/10.5194/acp-4111-4105-2011.

Huang, K., Zhuang, G., Lin, Y., Fu, J.S., Wang, Q., Liu, T., Zhang, R., Jiang, Y., Deng, C., Fu, Q., Hsu, N.C., Cao, B., 2012a. Typical types and formation mechanisms of haze in an Eastern Asia megacity, Shanghai. Atmospheric Chemistry and Physics 12, 105–124. http://dx.doi.org/10.5194/acp-12-105-2012.

Huang, K., Zhuang, G., Lin, Y., Wang, Q., Fu, J.S., Zhang, R., Li, J., Deng, C., Fu, Q., 2012b. Impact of anthropogenic emission on air-quality over a megacity – revealed from an intensive atmospheric campaign during the Chinese Spring Festival. Atmospheric Chemistry and Physics 12, 11631–11645. http://dx.doi.org/10.5194/acp-12-11631-2012.

Huang, K., Zhuang, G., Lin, Y., Wang, Q., Fu, J.S., Fu, Q., Liu, T., Deng, C., 2013. How to improve the air quality over mega-cities in China? – Pollution characterization and source analysis in Shanghai before, during, and after the 2010 World Expo. Atmospheric Chemistry and Physics, 5927–5942. http://dx.doi.org/10.5194/acp-13-5927-2013.

Huang, K., Zhuang, G.S., Xu, C., Wang, Y., Tang, A.H., 2008. The chemistry of the severe acidic precipitation in Shanghai, China. Atmospheric Research 89, 149–160.

Kaiser, D.P., Qian, Y., 2002. Decreasing trends in sunshine duration over China for 1954–1998: indication of increased haze pollution? Geophysical Research Letters 29 (21) http://dx.doi.org/10.1029/2002gl016057.

Kang, C.-M., Lee, H.S., Kang, B.-W., Lee, S.-K., Sunwoo, Y., 2004. Chemical characteristics of acidic gas pollutants and PM2.5 species during hazy episodes in Seoul, South Korea. Atmospheric Environment 38, 4749–4760.

Kleeman, M.J., Eldering, A., Hall, J.R., Cass, G.R., 2001. Effect of emissions control programs on visibility in southern California. Environmental Science & Technology 35, 4668–4674.

Lin, Y., Huang, K., Zhuang, G., Fu, J.S., Xu, C., Shen, J., Chen, S., 2013. Air quality over the Yangtze River Delta during the 2010 Shanghai Expo. Aerosol and Air Quality Research 13, 1655–1666. http://dx.doi.org/10.4209/aaqr.2012.11.0312.

Lott, N., 2004. The quality control of the integrated surface hourly database. In: 14th Conference on Applied Climatology, Asheville, NC, 15 January 2004. https://ams.confex.com/ams/84Annual/techprogram/paper_71929.htm.

Malm, W.C., Sisler, J.F., Huffman, D., Eldred, R.A., Cahill, T.A., 1994. Spatial and seasonal trends in particle concentration and optical extinction in the United States. Journal of Geophysical Research 99, 1347–1370. http://dx.doi.org/10.1029/93jd02916.

Schaap, M., Spindler, G., Schulz, M., Acker, K., Maenhaut, W., Berner, A., Wieprecht, W., Streit, N., Muller, K., Bruggemann, E., Chi, X., Putaud, J.P., Hitzenberger, R., Puxbaum, H., Baltensperger, U., ten Brink, H., 2004. Artefacts in the sampling of nitrate studied in the "INTERCOMP" campaigns of EUROTRAC-AEROSOL. Atmospheric Environment 38, 6487–6496. http://dx.doi.org/10.1016/j.atmosenv.2004.08.026.

Schichtel, B.A., Husar, R.B., Falke, S.R., Wilson, W.E., 2001. Haze trends over the United States, 1980–1995. Atmospheric Environment 35, 5205–5210.

Streets, D.G., Yu, C., Wu, Y., Chin, M., Zhao, Z., Hayasaka, T., Shi, G., 2008. Aerosol trends over China, 1980–2000. Atmospheric Research 88, 174–182.

Shanghai Statistical Yearbook, August, 2013. Atmospheric Environment Protection (1995–2012) (Chapter 6.15). China Statistics Press.

Smith, A., Lott, N., Vose, R., 2011. The integrated surface database recent developments and partnerships. Bulletin of the American Meteorological Society 92, 704–708. http://dx.doi.org/10.1175/2011bams3015.1.

Tao, J., Ho, K.F., Chen, L.G., Zhu, L.H., Han, J.L., Xu, Z.C., 2009. Effect of chemical composition of PM2.5 on visibility in Guangzhou, China, 2007 spring. Particuology 7, 68–75.

UNEP, 2009. UNEP Environmental Assessment: Expo 2010-Shanghai, China.

Vautard, R., Yiou, P., van Oldenborgh, G.J., 2009. Decline of fog, mist and haze in Europe over the past 30 years. Nature Geoscience 2, 115–119. http://dx.doi.org/10.1038/ngeo414.

Vinzani, P.G., Lamb, P.J., 1985. Temporal and spatial visibility variations in the Illinois vicinity during 1949–80. Journal of Climate and Applied Meteorology 24, 435–451. http://dx.doi.org/10.1175/1520-0450(1985)024.

Wang, J.L., Zhang, Y.H., Shao, M., Liu, X.L., Zeng, L.M., Cheng, C.L., Xu, X.F., 2006a. Quantitative relationship between visibility and mass concentration of PM2.5 in Beijing. Journal of Environmental Sciences (China) 18 (3), 475–481.

Wang, K., Dickinson, R.E., Liang, S., 2009. Clear sky visibility has decreased over land globally from 1973 to 2007. Science 323, 1468–1470.

Wang, S., Xing, J., Jang, C., Zhu, Y., Fu, J.S., Hao, J., 2011. Impact assessment of ammonia emissions on inorganic aerosols in East China using response surface modeling technique. Environmental Science & Technology 45, 9293–9300.

Wang, Y., Zhuang, G.S., Zhang, X.Y., Huang, K., Xu, C., Tang, A.H., Chen, J.M., An, Z.S., 2006b. The ion chemistry, seasonal cycle, and sources of PM2.5 and TSP aerosol in Shanghai. Atmospheric Environment 40, 2935–2952.

Watson, J.G., 2002. Visibility: science and regulation. Journal of the Air & Waste Management Association 52 (6), 628–713.

Yang, L.X., Wang, D.C., Cheng, S.H., Wang, Z., Zhou, Y., Zhou, X.H., Wang, W.X., 2007. Influence of meteorological conditions and particulate matter on visual range impairment in Jinan, China. Science of the Total Environment 383, 164–173.

Yuan, H., Wang, Y., Zhuang, G., 2003. Simultaneous determination of organic acids, methanesulfonic acid and inorganic anions in aerosol and precipitation samples by ion chromatography. Journal of Instrumental Analysis 22, 11–14.

Zhao, B., Wang, P., Ma, J.Z., Zhu, S., Pozzer, A., Li, W., 2012. A high-resolution emission inventory of primary pollutants for the Huabei region, China. Atmospheric Chemistry and Physics 12, 481–501. http://dx.doi.org/10.5194/acp-12-481-2012.

Zhuang, G.S., Guo, J.H., Yuan, H., Zhao, X.J., 2001. The compositions, sources, and size distribution of the dust storm from China in spring of 2000 and its impact on the global environment. Chinese Science Bulletin 46, 895–901. http://dx.doi.org/10.1007/Bf02900460.